Faraday Rotation Estimation Performance Analysis

Jun Su Kim & Konstantinos P. Papathanassiou
German Aerospace Center (DLR), Microwaves and Radar Institute (HR), Germany

Abstract

Different Faraday Rotation (FR) estimators are discussed, their estimation performances are assessed and compared to each other. The algorithms are applied on a set of quad-pol ALOS Pal-SAR data and the obtained estimates are validated against FR values derived from TEC maps obtained from GPS measurements.

1 Introduction

The current interest in low frequency space-borne SAR missions for vegetation monitoring makes compensation of the ionospheric impact on each measurements of crucial importance. The Earth's ionosphere impacts the polarised EM pulse transmitted/received by a SAR sensor in different ways and critically affects the quality of the obtained images. One of the prominent ionospheric distortions is Faraday rotation that appears as a direct consequence of the ionospheric birefringence induced by the presence of the Earth's magnetic field. The polarisation ellipse of the wave rotates as the wave propagates through the ionospheric layer. The scattering matrix of the underlying scattering process is distorted biasing the individual scattering amplitudes and phases.

The individual FR estimators proposed in the literature [1-4] can be divided into two categories: ones based on elements of the 2x2 complex scattering matrix [S] such as the Bickel & Bates estimator [1] and the (first) estimator proposed by Freeman [2], and methods based on second order elements of the polarimetric covariance (or coherency) matrix such as the second estimator proposed by Freeman in [2], the estimator proposed by Qi & Jin in [3] and more recently the estimator proposed by Chen & Quegan [4].

In this paper the estimation performance of the different Faraday Rotation (FR) estimators on quad-pol ALOS Pal-SAR data is discussed. As reference, global Total Electron Content (TEC) maps from the IONEX database obtained from the routine evaluation of dual-frequency GPS tracking data provided by the International GPS Service for Geodynamics (IGS). The TEC maps have a spatial resolution of 5° in longitude and 2.5° in latitude and a temporal resolution of 2 hours (RMS between 2 and 5 TECU).

2 Scattering & Covariance

The FR distortion of an underlying scattering matrix $[\mathbf{S}]$ is expressed by

$$[\mathbf{S}(\Omega)] = [\mathbf{R}_2(\Omega)][\mathbf{S}][\mathbf{R}_2(\Omega)] \quad (1)$$

where $[\mathbf{S}(\Omega)]$ is the measured (distorted) scattering matrix, $[\mathbf{R}_2(\Omega)]$ the (real) line-of-sight rotation matrix

$$\mathbf{R}_2 = \begin{pmatrix} \cos\Omega & \sin\Omega \\ -\sin\Omega & \cos\Omega \end{pmatrix} \quad (2)$$

where Ω is the one-way FR rotation angle. FR is invariant to the direction of wave propagation, but is dependent on the TEC level and on the orientation of the travelling direction of the wave relative to the Earth's magnetic field vector. It reaches its maximum at mid-latitudes and decreases towards high (due to the low TEC) and low (due to the advantageous orientation) latitudes. From Eq. (1) follows

$$\begin{aligned} S_{hh}(\Omega) &= +\cos^2(\Omega)\ \ S_{hh} - \sin^2(\Omega)\ \ S_{vv} \\ S_{hv}(\Omega) &= +\cos(\Omega)\sin(\Omega)\ \ (S_{hh} + S_{vv}) + S_{xx} \\ S_{vh}(\Omega) &= -\sin(\Omega)\cos(\Omega)\ \ (S_{hh} + S_{vv}) + S_{xx} \\ S_{vv}(\Omega) &= -\sin^2(\Omega)\ \ S_{hh} + \cos^2(\Omega)\ \ S_{vv} \end{aligned} \quad (3)$$

Note that in the presence of FR the measured scattering matrix $[\mathbf{S}(\Omega)]$ is no longer reciprocal i.e. $S_{hv}(\Omega) \neq S_{vh}(\Omega)$ even if the underlying scattering matrix $[\mathbf{S}]$ has $S_{hv} = S_{vh} = S_{xx}$.

The polarimetric covariance [C] matrix is defined by

$$[\mathbf{C}] = \left\langle \vec{k} \cdot \vec{k}^{*T} \right\rangle \text{, where } \vec{k} = \left(S_{hh}, S_{hv}, S_{vh}, S_{vv}\right)^T \quad (4)$$

is the 4-dim lexicographic scattering. [C] is by definition a 4x4 Hermitian positive semi-definite matrix. Eq. (1) can be rewritten in terms of the scattering vector as

$$\vec{k}(\Omega) = [\mathbf{R}_4(\Omega)]\vec{k} = \begin{pmatrix} C & -X & X & -S \\ X & C & S & X \\ -X & S & C & -X \\ -S & -X & X & C \end{pmatrix} \begin{pmatrix} S_{hh} \\ S_{xx} \\ S_{xx} \\ S_{vv} \end{pmatrix}$$

where $\vec{k}(\Omega)$ is the measured (distorted) scattering vector and $[\mathbf{R}_4(\Omega)]$ is the (real) 4x4 Faraday rotation matrix with $C := \cos^2\Omega$, $S := \sin^2\Omega$ and $X := \cos\Omega\sin\Omega$. The distorted covariance matrix follows

$$[\mathbf{C}(\Omega)] = \left\langle \vec{k}(\Omega) \cdot \vec{k}(\Omega)^{*T} \right\rangle = [\mathbf{R}(\Omega)_4][\mathbf{C}][\mathbf{R}(\Omega)_4]^T \quad (5)$$

The elements of $[\mathbf{C}(\Omega)]$ can be found to be

$$[\mathbf{C}(\Omega)] = \begin{pmatrix} C_{11} & C_{12} & C_{13} & C_{14} \\ C_{12}^* & C_{22} & C_{23} & C_{24} \\ C_{13}^* & C_{23}^* & C_{33} & C_{34} \\ C_{14}^* & C_{24}^* & C_{34}^* & C_{44} \end{pmatrix}. \quad (6)$$

Assuming reflection symmetric scatterers i.e. $\langle S_{hh} S_{xx}^* \rangle = \langle S_{xx} S_{vv}^* \rangle = 0$ the four diagonal (real) elements are given by [5]

$$\begin{aligned} C_{11} &= C^2 \rho_{HH} - 2CS\Re\{\rho_{HV}\} + S^2 \rho_{VV} \\ C_{44} &= S^2 \rho_{HH} - 2CS\Re\{\rho_{HV}\} + C^2 \rho_{VV} \\ C_{22} &= X^2 (\rho_{HH} + 2\Re\{\rho_{HV}\} + \rho_{VV}) + \rho_{XX} \\ C_{33} &= X^2 (\rho_{HH} + 2\Re\{\rho_{HV}\} + \rho_{VV}) + \rho_{XX} \end{aligned} \quad (7a)$$

and the six off-diagonal elements are given by

$$\begin{aligned} C_{12} &= CX\rho_{HH} + X(C\rho_{HV} - S\rho_{HV}^*) - SX\rho_{VV} \\ C_{13} &= -CX\rho_{HH} - X(C\rho_{HV} - S\rho_{HV}^*) + SX\rho_{VV} \\ C_{14} &= -CS\rho_{HH} + C^2 \rho_{HV} + S^2 \rho_{HV}^* - CS\rho_{VV} \\ C_{23} &= -X^2 (\rho_{HH} + 2\Re\{\rho_{HV}\} + \rho_{VV}) + \rho_{XX} \\ C_{24} &= -SX\rho_{HH} + X(C\rho_{HV} - S\rho_{HV}^*) + CX\rho_{VV} \\ C_{34} &= SX\rho_{HH} - X(C\rho_{HV} - S\rho_{HV}^*) - CX\rho_{VV} \end{aligned} \quad (7b)$$

where $\rho_{HH} = \langle S_{hh} S_{hh}^* \rangle$, $\rho_{HV} = \langle S_{hh} S_{vv}^* \rangle$, $\rho_{VV} = \langle S_{vv} S_{vv}^* \rangle$ and $\rho_{XX} = \langle S_{xx} S_{xx}^* \rangle$.

3 Faraday Rotation Estimators

The two most prominent FR estimators based on the scattering matrix elements are:

1. Bickel & Bates FR Estimator: The Bickel & Bates FR Estimator takes advantage of the fact that the eigenstates of the ionosphere are circular polarized waves that propagate with different velocities through the ionosphere. Accordingly, first the measured scattering matrix (in the linear H-V basis) is transformed into the L-R circular basis [6]

$$[\mathbf{S}_{\mathrm{LR}}(\Omega)] = \begin{pmatrix} 1 & \mathrm{i} \\ \mathrm{i} & 1 \end{pmatrix} [\mathbf{S}(\Omega)] \begin{pmatrix} 1 & \mathrm{i} \\ \mathrm{i} & 1 \end{pmatrix} \quad (8)$$

where FR is estimated from the phase difference between the (off-diagonal) LR-RL channels

$$\Omega = \frac{1}{4} \arg(\mathrm{S}_{\mathrm{LR}} \mathrm{S}_{\mathrm{RL}}^*). \quad (9)$$

Multi-looking of $\mathrm{S}_{\mathrm{LR}}\mathrm{S}_{\mathrm{RL}}^*$ can be written in terms of covariance matrix elements. The scattering vector $\vec{\mathrm{k}}_{\mathrm{LR}}$ in the circular basis is from Eq. (8),

$$[C_{LR}(\Omega)] = [\mathbf{I}_L^C][C(\Omega)][\mathbf{I}_L^C]^{*T} \quad [\mathbf{I}_L^C] = \begin{pmatrix} 1 & i & i & -1 \\ i & 1 & -1 & i \\ i & -1 & 1 & i \\ -1 & i & i & 1 \end{pmatrix} \quad (10)$$

where $[\mathbf{I}_{\mathrm{L}}^{\mathrm{C}}]$ is the 4x4 basis transformation operator. From Eq. (10) it follows that

$$\begin{aligned} \langle \mathrm{S}_{\mathrm{LR}} \mathrm{S}_{\mathrm{RL}}^* \rangle &= (\mathrm{C}_{11} + \mathrm{C}_{14} + \mathrm{C}_{41} + \mathrm{C}_{44} + \mathrm{C}_{23} + \mathrm{C}_{32}) - (\mathrm{C}_{22} + \mathrm{C}_{33}) \\ &\quad + \mathrm{i}(\mathrm{C}_{31} + \mathrm{C}_{13} + \mathrm{C}_{43} + \mathrm{C}_{34}) - \mathrm{i}(\mathrm{C}_{21} + \mathrm{C}_{12} + \mathrm{C}_{42} + \mathrm{C}_{24}) \end{aligned}$$

Using Eq. (7) and Eq. (12) it follows that

$$\langle \mathrm{S}_{\mathrm{LR}} \mathrm{S}_{\mathrm{RL}}^* \rangle = (\cos 4\Omega + \mathrm{i} \sin 4\Omega)(\rho_{\mathrm{HH}} + 2\Re\{\rho_{\mathrm{HV}}\} + \rho_{\mathrm{VV}}). \quad (13)$$

2. Freeman's FR Estimator: Freeman's scattering matrix estimator is based on the distortion of reciprocity in the presence of FR

$$\Omega = \frac{1}{2} \tan^{-1} \frac{\mathrm{S}_{\mathrm{hv}}(\Omega) - \mathrm{S}_{\mathrm{vh}}(\Omega)}{\mathrm{S}_{\mathrm{hh}}(\Omega) + \mathrm{S}_{\mathrm{vv}}(\Omega)}. \quad (14)$$

with nominator $\mathrm{S}_{\mathrm{hv}}(\Omega) - \mathrm{S}_{\mathrm{vh}}(\Omega) = (\mathrm{S}_{\mathrm{hh}} + \mathrm{S}_{\mathrm{vv}}) \sin 2\Omega$ and denominator $\mathrm{S}_{\mathrm{hh}}(\Omega) + \mathrm{S}_{\mathrm{vv}}(\Omega) = (\mathrm{S}_{\mathrm{hh}} + \mathrm{S}_{\mathrm{vv}}) \cos 2\Omega$. Note that the right hand side of Eq. (14) is not guaranteed to be real and that the ratio formation increases complexity for multilooking analysis of an analytical form of the [C] matrix.

Three popular FR estimators based on the covariance matrix elements are:

1. Freeman's Second (Covariance Matrix) FR Estimator is a modification of the scattering matrix formulation of Eq. (14) that can be rewritten as

$$\tan 2\Omega = \frac{S_{hv}(\Omega) - S_{vh}(\Omega)}{S_{hh}(\Omega) + S_{vv}(\Omega)}. \quad (15)$$

Multiplying both sides with their conjugates and performing (spatial) averaging yields:

$$\Omega = \frac{1}{2} \tan^{-1} \sqrt{\frac{\langle |S_{hv}(\Omega) - S_{hv}(\Omega)|^2 \rangle}{\langle |S_{hh}(\Omega) + S_{vv}(\Omega)|^2 \rangle}}. \quad (16)$$

The numerator is $C_{22} - C_{23} - C_{32} + C_{33}$ and the denominator is $C_{11} + C_{14} + C_{41} + C_{44}$ using the definition of covariance matrices in Eq. (4) and Eq. (6). If the diagonal terms are affected by noise this estimator is expected to over-estimate FR.

Because Eq. (16) is quadratic, the sign of Faraday rotation cannot be determined.

Freeman's 2nd estimator can be analyzed by the replacing covariance matrix with Eq. (7). The denominator of Eq. (16) is $\cos^2 2\Omega (\rho_{HH} + 2\Re\{\rho_{HV}\} + \rho_{VV})$ and the numerator is $\sin^2 2\Omega (\rho_{HH} + 2\Re\{\rho_{HV}\} + \rho_{VV})$. We can see again the separation of amplitude terms and phase (FR) terms.

2. Qi & Jin FR Estimator: Qi & Jin introduced a FR estimator based on the distorted covariance matrix elements

$$\tan 2\Omega = \frac{\Im\{C_{12} - C_{13}\}}{\Im\{C_{14}\}}. \quad (17)$$

Using Eq. (7), the numerator equals $\Im\{\rho_{HV}\} \sin 2\Omega$ and the denominator to $\Im\{\rho_{HV}\} \cos 2\Omega$.

3. Quegan & Chen FR Estimator: More recently, Quegan & Chen proposed an alternate FR estimator (more accurately six different estimators) based on the

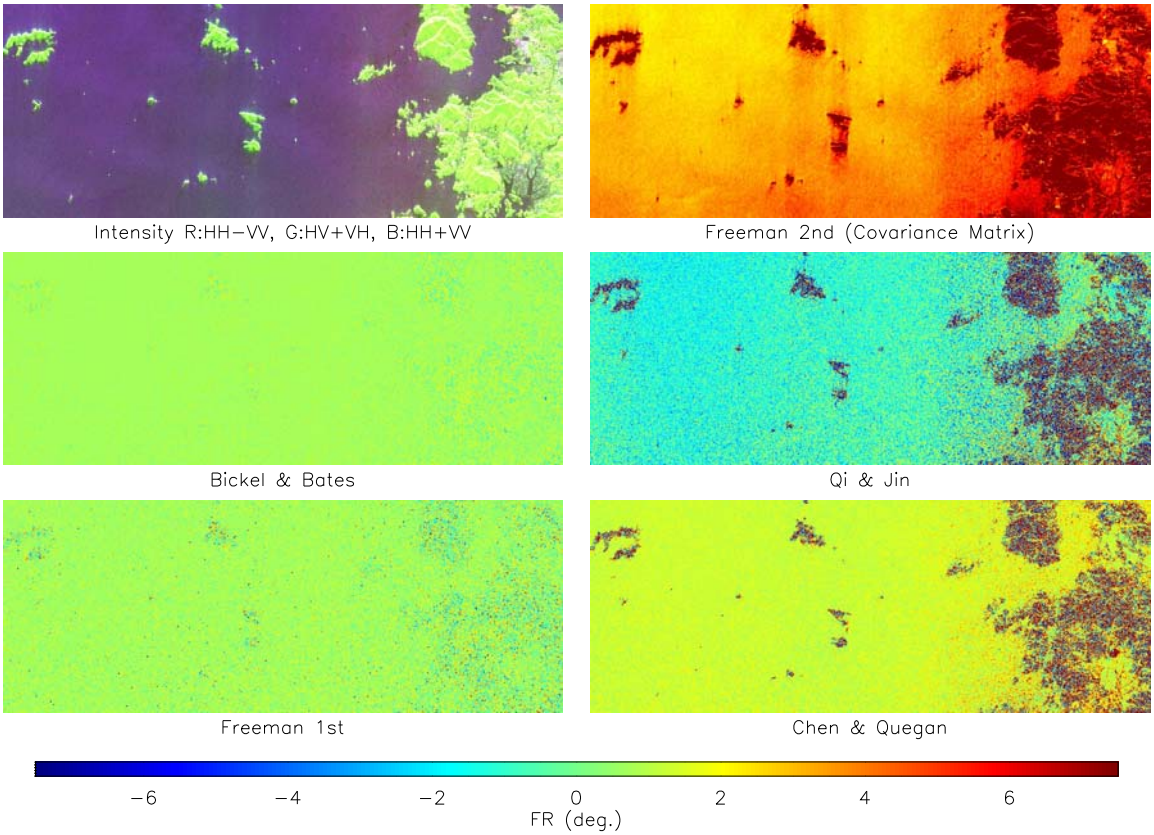

Figure 1: FR maps obtained by the five estimators over an ALOS-PalSAR scene of Korean coastline. (4 by 24 look)

covariance matrix elements. The one with the best performance is given as

$$\Omega = \arg\left(\Im\{C_{14}\} + i\Im\{C_{12} + C_{23} - C_{13} - C_{34}\}/2\right). \quad (18)$$

Eq. (18) is similar to the Qi & Jin estimator. Note that $\Im\{\rho_{HV}\} = \Im\{C_{12} - C_{13}\} = \Im\{C_{23} - C_{34}\}$ in the absence of noise. They differ only in the presence of noise. The sum of two redundant terms in the imaginary part reduces noise effects for the Quegan & Chen estimator. Note that while the Quegan & Chen estimator uses the argument of a complex number that allows estimation in $[-\pi, \pi]$, the Qi & Jin estimator uses the tangent function with estimation in $[-\pi/2, \pi/2]$.

Finally, note that because both transmitted and received pulses travel through the ionosphere [S] is affected by the 2-way ionospheric distortion so that FR estimates are always by estimates of 2Ω confining the estimation of Ω to $[-\pi/2, \pi/2]$ or $[-\pi/4, \pi/4]$.

4 ALOS PalSAR

The estimation performance of each algorithm is assessed on ALOS PalSAR data. For this we used different test sites located in the northern as well as on the southern hemisphere that cover a small but still significant range of 4 degrees FR (-1.5° to 2.5°) with very different scattering (sea ice, savanna forest, open sea etc.) and terrain characteristics. Figure 1 shows the FR maps obtained from the five FR estimators for a scene over the vegetated coastline of Korea as an example. The reference FR form IONEX data is 2.6° (a rather poor estimate in this case). One important point is the dependency of the estimation performance - especially of the covariance matrix based approaches - on the scattering characteristics of the scene which becomes evident in the estimation results in Figure 1. All three covariance matrix based approaches provide different FR estimates (and/or performances) over the sea than over the (forested) islands. The Qi & Jin and Chen & Quegan estimators depend on ρ_{HV} which is scattering dependent. Accordingly, the performance of these two estimators

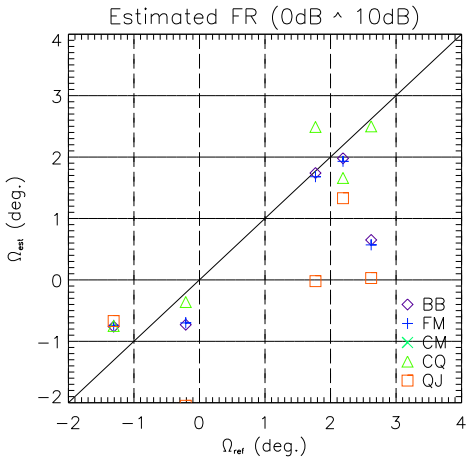

Figure 2: Estimated vs. Reference FR of the five estimates. BB: Bickel & Bates, FM: Freeman's 1st, CM: Freeman's 2nd, CQ: Chen & Quegan, QJ: Qi & Jin. The absence of CM points is due to their strong overestimation.

degrades over areas dominated by volume scattering (i.e. vegetated terrain).

Figure 2 shows the obtained correlation between the mean estimated FR obtained from the various estimators and the reference FR derived from the IONEX TEC values and using the World Magnetic Model (WMM). The estimation performance varies significantly among the individual estimators and depends on the scene scattering characteristics. Note that the accuracy (and resolution) of the reference TEC maps only allows a rather rough evaluation.

The full comparison performed cannot be included in this paper due to the limitation of space and will be presented at the conference. However, the analysis can be summarized by following points:

1. In general the scattering matrix based estimators show better results than the covariance matrix approaches.
2. Among the covariance matrix based estimators the Chen & Quegan estimator shows the best performance. Freeman's 2nd estimator leads to strongly over-estimated FR values.
3. The (mean) FR estimates are widely robust against SNR effects. An exception is Freeman's 2nd estimator which overestimates FR except in the case of a high SNR.
4. The lowest standard deviation σ_Ω for the estimated FR is obtained using the Bickel & Bates estimator followed by Freeman's 1st estimator. σ_Ω values are in general larger using the covariance matrix based estimators (for an equivalent number of looks). Chen & Quegan's estimator shows the better performance among the three covariance matrix based estimators.

5 TEC Estimation

As FR is proportional to TEC, the estimation of FR allows an estimation of TEC according to [6], [7]

$$\mathrm{TEC} = \frac{mcf^2 \cos\theta}{\varsigma e \vec{B}\cdot\hat{\kappa}}\Omega \qquad (19)$$

where m and e are the electron mass and charge respectively, $\varsigma = e^2/8\pi^2\varepsilon_0 m = (c^2/2\pi)r_e$ =40.30818773 m^3/s^2 with r_e the classical electron radius, $\vec{B}$ is the Earth's magnetic field, $\hat{\kappa}$ the wave vector and θ the incidence angle. At mid-latitudes ($\vec{B}\cdot\hat{\kappa} \approx 3.0\times10^{-5}$T), 1° of FR corresponds at L-band to 3.8 TECU. At P-band 1° FR corresponds to 0.43 TECU revealing the potential of using FR estimates to estimate TEC. On the other hand, FR estimates at P-band may have to be unwrapped in order to provide absolute TEC: at mid-latitudes, the $\pi/2$ FR ambiguity corresponds to 340 TECU at L-band but only 39 TECU at P-band. This means 19.5 TECU lead to $\pi/4$ FR (at P-band). A global map of TEC levels (in TECU) corresponding to $\pi/4$ FR at P-band is shown in Figure 3.

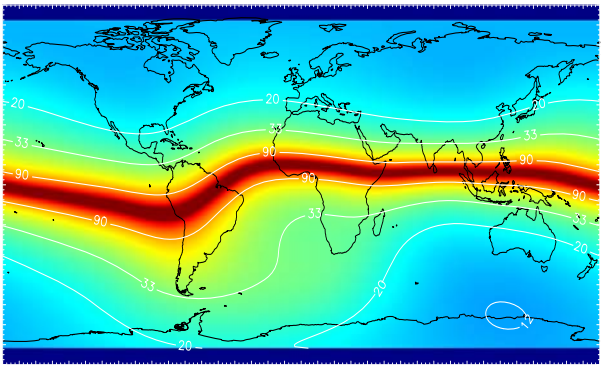

Figure 3: TEC (in TECU) corresponding to $\pi/4$ FR at P-band.

6 Conclusion

Five Faraday Rotation (FR) estimators have been discussed. The algorithms have been applied on a set of quad-pol ALOS Pal-SAR data and the obtained estimates are validated against FR values derived from TEC maps obtained from GPS measurements. The obtained estimation performance varies significantly between the individual estimators and depends additionally on the scene scattering characteristics.

References

[1] S. H. Bickel and R. H. T. Bates, "Effects of magnetoionic propagation on the polarisation scattering matrix," *proc. IEEE,* vol. 53, no. 8, pp. 1089-1091, Aug. 1965.

[2] A. Freeman, "Calibration of Linearly polarized polarimetric SAR data subject to Faraday rotation," *IEEE Transactions of Geoscienc3 and Remote Sensing,* Vol. 42, no. 8, pp. 1617-1624, Aug. 2004.

[3] R. Y. Qi and Y.-Q. Jin, "Analysis of the effects of Faraday rotation on spaceborne polarimetric SAR observations at P-band," *IEEE transactions of Geoscience and Remote Sensing,* Vol. 45, no. 5, pp. 1115-1122, May 2007.

[4] J. Che and S. Quegan, "Improved estimators of Faraday rotation in spaceborne polarimetric SAR data," 2009, unpublished.

[5] A. Freeman and S. S. Saatchi, "On the detection of Faraday Rotation in Linearly polarized L-band SAR Backscatter Signatures", *IEEE transactions of Geoscience and Remote Sensing,* Vol. 42, no. 8, pp. 1607-1616, Aug. 2004.

[6] F. J. Meyer and J. B. Nicoll, "Prediction, Detection and Correction of Faraday Rotation in Full-Polarimetric L-Band SAR Data", *IEEE transactions of Geoscience and Remote Sensing,* Vol. 46, no. 10, pp. 3076-3086, Oct. 2008.

[7] D. P. Belcher, "Theoretical limits on SAR imposed by the ionosphere", *IET Radar Sonar Navig.*, Vol. 2, No 6, pp. 435-448, 2008, doi: 10.1049/iet-rsn:20070188